

GALEX ULTRAVIOLET OBSERVATIONS OF STELLAR VARIABILITY IN THE HYADES AND PLEIADES CLUSTERS

STANLEY E. BROWNE,^{1,2} BARRY Y. WELSH,^{1,2} AND JONATHAN WHEATLEY²

Draft 2009 March 31st, Submitted to PASP

ABSTRACT

We present *GALEX* near ultraviolet (NUV:1750 - 2750Å) and far ultraviolet (FUV: 1350 - 1750Å) imaging observations of two 1.2° diameter fields in the Hyades and Pleiades open clusters in order to detect possible UV variability of the member stars. We have performed a detailed software search for short-term UV flux variability during these observations of the ~ 400 sources detected in each of the Hyades and Pleiades fields to identify flare-like (dMe) stellar objects. This search resulted in the detection of 16 UV variable sources, of which 13 can be directly associated with probable M-type stars. The other UV sources are G-type stars and one newly discovered RR Lyrae star, USNOB1.0 1069-0046050, of period 0.624 d and distance ~ 4.5 to 7 kpc. Light curves of photon flux versus time are shown for 7 flare events recorded on six probable dMe stars. UV energies for these flares span the range 2×10^{27} to 5×10^{29} erg, with a corresponding variability change of $\Delta\text{NUV} = 1.82$ mag. Only one of these flare events (on the star Cl* Melotte 25 LH129) can definitely be associated with an origin on a member the Hyades cluster itself. Finally, many of our M-type candidates show long periods of enhanced UV activity but without the associated rapid increase in flux that is normally associated with a flare event. However, the total UV energy output during such periods of increased activity is greater than that of many short-term UV flares. These intervals of enhanced low-level UV activity concur with the idea that, even in quiescence, the UV emission from dMe stars may be related to a superposition of many small flare events possessing a wide range of energies.

Subject headings: stars, star clusters

1. INTRODUCTION

M-dwarf stars are the dominant stellar component of our Galaxy by number, comprising more than 70% of the stellar population in the solar neighborhood. They are almost fully convective with intense magnetic fields covering most of their stellar disk, and are thus good astrophysical laboratories for the study of the more extreme cases of magnetic processes (both coronal & chromospheric) that occur in the outer atmospheres of other (more quiescent) stars such as our Sun. Recently, their importance as a major reservoir of stellar hosts for planetary systems has been realized, and thus estimating the physical conditions and size of a ‘habitability zone’ around such UV/X-ray active stars is of great value in assessing whether M-star planetary systems are capable of sustaining living organisms (Segura et al. 2005). Such a determination is directly linked to the stellar activity levels and the associated flare energies expected from each spectral class of M-star. These numbers, unfortunately, are presently poorly known at both X-ray and UV wavelengths.

Much of our knowledge of the long-term evolution of stellar coronal activity derives from X-ray observations of open clusters (Stern et al. 1995). These stellar associations constitute a large sample of coeval stars with a similar distance and similar chemical composition, thus providing us with a powerful tool for a statistical study of the behavior of magnetically active stars. Comparison studies show that X-ray emission decreases from younger to older clusters, and this decrease in coronal activity with age may be due to rotational spin-down caused by magnetic breaking. However, the influence of (often unknown) binary companions in such systems complicates this interpretation, and therefore most X-ray studies have been observationally biased towards highly active (and nearby) stars,

such that slowly rotating stars with relatively weak X-ray activity (i.e. late M-dwarfs) are generally unaccounted for. The majority of X-ray observations often cannot reveal flux variability on time-scales < 500 sec (Pillitteri et al. 2005), which biases such results against a flux contribution from the (more numerous) weakly X-ray flaring dMe stars. This point is highlighted by the *XMM* observations of Proxima Cen (dM5.5e) in which varying low-level emission activity ($E \sim 10^{28}$ erg) was persistent over a period of 45ksec, prior to the onset of a far larger (and easily more detectable) X-ray flare event (Gudel et al. 2004). It has even been suggested that no real quiescence may be present at all in X-ray coronae, such that the observed emission may be produced by a superposition of multiple lower energy flares (Gudel et al. 2003). Recent multi-wavelength observations of stellar flares have also revealed an astounding lack of correlation between flares seen in different wavelength regions (Osten et al. 2005), with UV flares on HR 1099 showing little or no change in the coronal (X-ray) emission, whereas the UV line-shapes broadened appreciably (Ayes et al. 2001).

Over the past 5 years the NASA Galaxy Evolution Explorer (*GALEX*) satellite has been carrying out both far UV (FUV: 1350 - 1750Å) and near UV (NUV: 1750 - 2750Å) broadband imaging observations of a large percentage of the sky (Martin et al. 2005). Although designed primarily for UV observations of low-*z* galaxies, the instrument is proving to be a powerful tool for the investigation of time-variable and transient stellar phenomena. For example, long-term (>1500 s) variability, as determined from comparisons of orbit-averaged UV magnitudes, has recently been reported for several hundred objects in the *GALEX* Ultraviolet Variability (GUVV) catalogs (Welsh et al. 2005; Wheatley et al. 2008). The majority of these UV variable sources have been shown to be active galaxies, but a non-significant fraction of the variable sources are galactic M-type stars. In a more extended search

¹ Eureka Scientific, 2452 Delmer Street, Oakland, CA 94602-3017

² Experimental Astrophysics Group, Space Sciences Laboratory, University of California, 7 Gauss Way, Berkeley, CA 94720. seb@ssl.berkeley.edu

of *GALEX* data for short-term variability, 49 NUV flare events occurring on time-scales < 150 seconds that can be associated with M-dwarf stars of distances 25 to 990 pc and with flare energies ranging from as low as 8×10^{27} and up to 1.6×10^{31} erg have been detected (Welsh et al. 2007). This range of NUV flare energy (and the associated flare light-curve behavior) is very similar to that recorded in the visible U-band for nearby ($d < 25$ pc) M-dwarfs (Panagia et al. 1995), which argues strongly for a common emission mechanism for both the U-band and *GALEX* NUV bands, i.e. that of continuum emission (Hawley et al. 2003). However, for flares recorded in the shorter wavelength FUV band, CIV line emission must become a major contributor to the observed flux.

In this Paper we continue our program of UV variability studies using *GALEX* with photometric imaging observations of two pairs of 1.2° diameter fields lying within the Hyades and Pleiades open clusters to investigate the FUV and NUV variability associated with magnetic activity in member M-dwarf stars. Due to the intrinsic high UV brightness of some of the stars in each cluster (which can cause saturation of the *GALEX* detectors), the two pairs of fields were offset by a few degrees from the nominal centers of each cluster. Both cluster fields contain several M-stars whose flaring signatures have previously been recorded at both X-ray and visible wavelengths (Stern et al. 1995; Mirzoyan et al. 1994; Hambaryan et al. 1997). The Hyades cluster lies at a mean distance of only 46 pc and with an age of ~ 625 Myr (Perryman et al. 1998), is probably the most well-studied of all open clusters, with about ~ 300 possible members extending over 20° on the sky. The more distant Pleiades cluster lies at ~ 135 pc (Soderblom et al. 2005) and has an estimated age of ~ 110 Myr with ~ 1400 probable members being listed within the central 6 sq. deg of the cluster (Stauffer et al. 2007). Although the average rotation rate for M stars in the Hyades is only 0.4 times that of the far younger and more active members of the Pleiades cluster, there is still a large number of Hyades M-dwarfs that exhibit appreciable chromospheric activity as revealed by H- α observations (Terndrup et al. 2000; Stauffer et al. 1997; Reid et al. 1995). X-ray observations of the Hyades with the *ROSAT* satellite have shown that $\sim 30\%$ of its 306 cataloged K and M-type stars are coronally active down to a limiting X-ray luminosity of 10^{28} erg s^{-1} (Stern et al. 1995). Similar X-ray observations of the Pleiades members resulted in almost all of the catalogued early dMe stars being detected down to a limiting X-ray luminosity of 3×10^{28} erg s^{-1} (Micela et al. 1996). All four of our selected fields for observation with *GALEX* contain numerous previously identified M-type Hyad and Pleiad members, thus providing us with the potential to detect several UV flares emitted from field M-dwarfs during each of the four $\sim 15,000$ s periods of observation. In the following sections we describe these observations and discuss the UV variable sources found in each field and present the UV flare signatures and associated flare energies for seven identified dMe stars.

2. *GALEX* UV IMAGING OBSERVATIONS

Two sky-fields in the Hyades cluster centered on (A) R.A.04:34:16, Dec.+17:08:56 (2000.) and (B) R.A.04:27:47, Dec+17:05:24 (2000.) were observed for a total of 15,989 s and 15,252 s respectively in both of the FUV and NUV imaging channels of the *GALEX* satellite (Martin et al. 2005). Similarly, two sky-fields in the Pleiades cluster centered on (A) R.A.03:44:20, Dec.+22:00:00 (2000.) and (B)

R.A.03:45:05, Dec.+26:20:00 (2000.) were observed for a total of 33,806 sec and 43,373 s respectively, but solely in the the *GALEX* NUV channel. In addition, one exposure of both of the Pleiades fields was recorded in the FUV channel for 1500 s only. All these data were recorded as time-tagged photon events by the *GALEX* micro-channel plate detectors (Morrissey et al. 2005; Morrissey et al. 2007). Each *GALEX* image has a diameter of $\sim 1.24^\circ$ on the sky and the total observation period for each field was split into 12 (Hyades) and 28 (Pleiades) separate exposures, each of approximately 1500 s duration (i.e. one *GALEX* orbital eclipse period). A few of the exposures were less than the nominal 1500 s duration due to satellite scheduling and instrumental constraints. Although most of the exposures were recorded consecutively, the actual observations are not contiguous due to a 60 minute gap between each exposure during which the *GALEX* detector high voltage is ramped down to avoid the daylight part of the satellite orbit. All these data were recorded as part of the NASA *GALEX* Guest Investigator Cycle 2 (ID: GI2-001) and Cycle 4 (ID:GI3-042) programs and the corresponding NUV and FUV images for each of the 4 sky-fields are shown in Figure 1. The appearance of these images is now briefly discussed.

2.1. *The UV images of the Hyades Fields (A) and (B)*

These two UV image fields, shown in the upper region of Figure 1, are at a similar Declination and are almost adjacent to each other in Right Ascension. The fields both lie $\sim 2.5^\circ$ from the nominal center of the cluster, which itself extends over $\sim 20^\circ$ on the sky. Due their proximity to the Sun ($d \sim 46$ pc), both of these Hyades UV images are essentially unaffected by the effects of interstellar gas or dust absorption. The brightest UV sources in both of these *GALEX* images are nearby ($d < 10$ pc) F and G-type field stars with a high proper motion. We note that both Hyad (and Pleiad) M-stars are intrinsically faint, and are generally only observable in the ultraviolet region due to their enhanced emission associated with chromospheric and transition region activity. Based on the previously known Hyades member stars that are contained within these two fields (Reid et al. 1995; Stauffer et al. 1997; Perryman et al. 1998), there are 4 M-type stars in Hyades-A and one in the Hyades-B field. However, we note that these three referenced studies are magnitude limited ground-based observations in which the intrinsically faint M-type stars (and those more distant than the Hyades cluster) may not be fully represented.

2.2. *The UV images of the Pleiades Fields-(A) and -(B)*

These two fields (shown in the lower region of Figure 1) lie approximately $\pm 1^\circ$ in Declination from the nominal center of the Pleiades cluster, whose stellar membership down to a limiting magnitude of $R \sim 20$ has been catalogued by Adams et al. (2001). Both of the *GALEX* UV images of the Pleiades fields appear dramatically different to those of the Hyades. Both Pleiad images reveal substantial nebular UV emission in the form of many filamentary structures formed by both interstellar scattering and reflection of radiation from the nearby UV-bright B-type cluster stars. Previous UV and IR studies of the Pleiades region by Gibson and Nordsieck (2003) have shown that the majority of the observed UV emission is from forward scattering of foreground interstellar dust grains.

The brightest stellar sources in both of the Pleiades UV images are, in common with the Hyades images, dominated by

nearby ($d < 10\text{pc}$) F and G-type stars. Using the positions of known M-type stars in these two fields, as listed by Adams et al. (2001) and J. Stauffer (private communication), there are 7 previously catalogued M-type stars in the Pleiades-(A) field and 10 M-type stars in the Pleiades-(B) field.

3. DATA REDUCTION

The photon data for each image exposure were processed using Version 5 of the *GALEX* Data Analysis Pipeline operated at the Caltech Science Operations Center, Pasadena, CA., (Morrissey et al. 2005). The final data product is a flat-field corrected photometric time sequence of photons positionally mapped in Right Ascension and Declination to the sky. The *GALEX* pipeline then utilizes the SExtractor program of Bertin & Arnouts (1996) for the detection and photometry of UV sources contained within each of these NUV and FUV photon image fields. This procedure produces a catalog of *GALEX* UV sources, which typically are brighter than NUV magnitude ~ 23.0 for a nominal 1500 s observation (Morrissey et al. 2005). However, due to edge-effects in the *GALEX* images we only used the data contained within the central 0.55° radius of each field for our subsequent scientific analysis of UV sources. In addition, the *GALEX* images are subject to a number of noise-producing signals (such as reflections from the edge of the detector) that are called ‘artifacts’ and many (but not all) are duly flagged in the quality assessment phase of data processing which we removed from our analysis. Also, the Pleiades images have many diffuse and extended features due to UV emission from foreground interstellar gas and dust, which can confuse the SExtractor source detection algorithm at the faintest detection levels. Thus, in order to reduced the number of ‘false’ UV source detections, we limited our search to sources brighter than NUV magnitude = 22.5 and to those sources with a measured *GALEX* point spread function of < 8 arcsec fwhm (i.e. stellar and not extended extragalactic sources). Our search procedure revealed that Hyades Field-A contained 335 UV stellar sources, Hyades Field-B contained 345 UV sources, Pleiades Field-A contained 323 UV sources and Pleiades Field-B contained 502 UV stellar sources.

The list of exposure-to-exposure NUV (and corresponding FUV) magnitudes for each of the previously identified UV sources, together with their associated ($1-\sigma$) measurement errors, was then queried to determine potential source variability for a given image field over the time series of observations. Statistically significant stellar variability, as opposed to variations in the background Poisson noise, was deemed to be real if the largest difference between the the set of source magnitude measurements exceeded $2 \times 1-\sigma$ measurement error (i.e. typically > 0.3 mag). This initial variability selection criterion was based on extensive searches of the *GALEX* archive that resulted in the assembly of the two GUVV catalogs (Welsh et al. 2005; Wheatley et al. 2008). Unfortunately, due to the presence of the many artifacts (listed previously) that affected the present *GALEX* images, the sole use of this statistical test in revealing low levels of source variability often produced many false positive detections. Hence, actual verification of the true long term variable nature of these sources required individual visual inspection of their stellar images (to reveal low count rate artifacts), in addition to a short statistical comparison of the source photon list data for each exposure. This latter statistical test on the photon data involved a comparison between the mean source count rate level (and its associated standard error) established for each

750s of every exposure (i.e. half an observation period). Stellar count rate variability was deemed significant in a similar manner to that established for the exposure-to-exposure magnitudes, in that the count rate level needed to exceed $2 \times 1-\sigma$ of the count rate standard error.

The application of these two selection criteria resulted in the identification of a total of 6 variable stellar Hyad candidates and 8 variable stellar Pleiad candidates. The UV variable sources found in each of the 4 observed fields are listed in Table 1 together with their galactic co-ordinates and their respective observed maximum and minimum FUV and NUV magnitudes ($FUV_{max/min}$, $NUV_{max/min}$). In cases where these sources have previous identifications in the Simbad database and/or they are listed in either the USNO-B1.0 (Monet et al. 1998) or the Two Micron All Sky Survey (2MASS) catalog (Cutri et al. 2003), these are also listed in Table 1 together with their 2MASS (H - K) and (J - H) color magnitudes.

As a check on finding (short-term) flaring and/or variable sources whose UV output may have changed over time intervals much shorter than one *GALEX* exposure (i.e. $<< 1500$ s), or with a small flux change that, over the integration of one exposure, may have been undetected by our exposure-to-exposure magnitude comparison method, we subsequently inspected the time-tagged photon list files for all of the UV sources present in each of the 4 image fields. Since this involves the inspection of a very large amount of data, we used a crude data compression method to inspect the photon data for all of the UV sources contained within each individual exposure. We used the ‘varpix’ variability search algorithm (Welsh et al. 2007), in which the software tool bins all of the photon data accumulated in consecutive 16 s time intervals over image areas of 12 arcsec^2 pixels for each exposure. Intensity variability for each of the these ‘super-pixels’ as a function of time throughout an exposure period is then assessed against the median and maximum photon flux value to determine a ‘variability signal-to-noise ratio’ for each of these large image pixels. We identified potential variable sources in our present images as those with a variability signal-to-noise ratio $> 8:1$. This ratio was chosen through a trial and error approach on several *GALEX* images in order to minimize the many false positives that occur at lower variability S/N ratios. These false variability detections at low S/N are caused by the flux from bright objects spilling over into adjacent ‘super-pixels’, thus causing the appearance of source variability. For S/N variability $> 8:1$, we deemed that if the variation in source flux was due to a flaring dMe star, then a characteristic flare light curve should emerge from an inspection of the ‘varpix’ output (Welsh et al. 2007). The ‘varpix’ search method confirmed all of our 14 previously detected variable sources, with the addition of one new flaring source, SDSS J0422842.78+171149.6, within the Hyades-B field.

For sources with only one detection over the entire series of exposures (i.e. transients), the previous statistical tests for variability were not applicable. We therefore set a criterion for the examination of all single detections of UV sources brighter than a limiting magnitude of $NUV < 23.0$. We then examined the photon list light curves for all of these selected sources using the ‘varpix’ software tool, which resulted in the discovery of one new source, Hyades-A 04:33:56.6 +16:52:09.6. From the application of all of these search methods we believe that no single UV (long and short-term) variable star brighter than NUV magnitude ~ 22.5 was missed in our present variability search, the results of which are listed

in Table 1.

4. RESULTS AND DISCUSSION

4.1. *The Identification of M-type Stars*

The particular topic of present interest is the enhanced levels of chromospheric and coronal activity on dMe stars that can produce large stellar flares which are observable at ultraviolet wavelengths. Therefore, we need to determine which of the UV variable objects listed in Table 1 can be directly associated with dMe flare stars. We note that most ground-based visual studies of stars seen towards both the Hyades and Pleiades clusters are magnitude limited observations in which the intrinsically faint M-type stars may not be fully represented (Perryman et al. 1998; Dobbie et al. 2002; Stauffer et al. 2007). Therefore, previous estimates of both the numbers of M-type stars and their possible membership status of both clusters are far from being complete. In addition, the fraction of chromospherically active M stars peaks at spectral type M7 (West et al. 2008), such stars often being too faint to be detected in many visible studies. Thus, without deep multi-band visible photometry and a measurement of stellar proper motion and stellar spectral type, obtaining accurate estimates of the number of all possible UV active M-type stars in either of our cluster fields (and their cluster membership status) is beyond the present scope of this paper.

Fortunately 2MASS photometric stellar magnitude data (as listed in Table 1) are available for both of our observed regions (Cutri et al. 2003), whereas Sloan Digital Sky Survey (SDSS) data are only available for a small area of one of the Hyades-B fields (York et al. 2000). Relationships between the SDSS and 2MASS color magnitudes have been derived for $\sim 38,000$ low-mass stars (West et al. 2008), and can be used to identify possible M-type stars. In Figure 2 we show the locus of a 2MASS (H - K) versus (J - H) color-color diagram that encompasses M0 to M9 spectral types (West et al. 2008). We also show the positions of the UV variable sources listed in Table 1. This figure clearly shows that 12 of our sample of UV variables lie in the region of the plot where M-type stars are to be expected to be found. Three of the 4 outlying objects lie to the left of the main grouping of Figure 2 and are thought not to be M-type stars. These non M-type stars are now briefly discussed in Section 4.2 prior to a more detailed discussion of the remaining 13 sources in Section 4.3, which we argue are probable M-type stars.

4.2. *Non M-type Hyades and Pleiades UV Variables*

4.2.1. *Hyades-B source 04:27:53.6 +16:51:36.0*

The ‘varpix’ light-curve for this object showed no sign of short-term variability that could be associated with flaring, but instead revealed the source to possess a near-constant level of increased emission measured during two exposures compared to that observed over other observation periods. Its 2MASS colors are more consistent with a star of spectral type F or G (Finlator et al. 2000), and we note that *ROSAT* observations of the Hyades revealed a high detection rate for known G-type stars and binary systems (Stern et al. 1995). Thus, the cause of the weak (and long duration) UV variability that we have observed for this object could possibly be due to the presence of a close companion star.

4.2.2. *Hyades-B source 04:28:32.4 +16:58:21.6*

Figure 3 shows the NUV light-curve for this source, which shows clear periodic variability with a maximum increase of

$\Delta\text{NUV} = 1.64$ mag. and $\Delta\text{FUV} > 2.76$ mag. This type of UV flux variation is very similar to that observed by *GALEX* for RR Lyrae stars (Wheatley et al. 2005), in which the stellar brightness variation is primarily due to radial pulsations that produce an observed temperature change that is mostly pronounced in the UV. Under the assumption of its RR Lyrae nature, we have derived a period of 0.624 d for this source, which is a typical value for this type of star.

Using a 2MASS K magnitude of 13.5, $E(B-V) = 0.38$ and the period-luminosity relation of Sollima et al. (2008) for RR Lyraes, we derive a distance of ~ 4.5 to 7 kpc for this star, placing it well out into the galactic halo.

4.2.3. *Pleiades-B source 03:42:59.0 +26:17:01.0*

The ‘varpix’ light-curve for this source revealed an increased level of UV emission during only a few orbits, with no obvious associated short-term flare signature. Its 2MASS colors are consistent with a star of spectral type earlier than G5 (Finlator et al. 2000), and *ROSAT* X-ray observations of the central region of the Pleiades cluster revealed a high detection rate for dwarf G-type stars (Micela et al. 1996). Since binary dG stars are more intense X-ray emitters than single dG-type stars, it seems probable that binarity may well be the cause of its observed UV variability.

4.3. *M-type Hyades and Pleiades UV Variables*

The following section discusses likely M-type stars that were detected as UV variables in both the Pleiades and Hyades fields. For the 6 stars that exhibited flaring signatures, we show their NUV light-curves (i.e. counts versus time) in Figure 4. Note that Pleiades-B source 03:43:35.5 +26:21:31.1 was observed flaring on two occasions. All flaring signatures were also detected in the FUV channel for both Hyades fields, but the photon data are of a much lower signal-to-noise ratio and are therefore not shown in Figure 4.

The UV light-curves of a sample of ~ 50 dMe flare stars observed with *GALEX* have been previously investigated (Welsh et al. 2007). The authors found 3 distinctive signatures of these flare events in plots of photon flux versus time (see Figure 2 of their paper), and the present NUV flare light-curves shown in our Figure 4 are all qualitatively consistent with those flare signatures.

Finally, we remind the reader that *GALEX* has an uneven observational cadence with at least a 60 minute gap between individual exposures. On certain occasions (due to satellite operational constraints) this gap was several hours long. Thus, although *GALEX* is an ideal detector of UV emission from both large and small flare events, it is not an ideal tracer of the time evolution of flares for periods longer than 1500 s. As such, these observations are not well suited for accurate determinations of flare activity rates recorded over time periods > 1500 s. In the following subsections we briefly discuss the UV variability detected on the M-type stars in both cluster fields.

4.3.1. *Hyades-A source 04:33:56.6 +16:52:09.6*

This was the only transient source detected by our variability search. It showed no conclusive UV flare signature in its ‘varpix’ light curve during the single exposure in which it was detected and it is listed with a spectral type of M1 in Simbad. It has been classified as a Hyades cluster member through proper motion studies (Reid 1992), and has also been detected at X-ray wavelengths (Stern et al. 1995). It is likely

that our detection of this source in the UV was caused by observing it after a large stellar flare which had yet to return to its low pre-flare flux level (which in this case was beneath the detection limit of *GALEX*). Another plausible explanation for the transient nature of this source could be the detection of UV emission from an eruptive binary companion star.

4.3.2. *Hyades-A source 04:34:31.3 +17:22:20.1*

This source showed no flaring signature in its ‘varpix’ light curves and its 2MASS colors are consistent with an M-type spectral classification. It has no previous history of flare activity, but was detected by *GALEX* in all of the 12 NUV exposures with the majority of detections lying in the $19.9 < \text{NUV} < 20.3$ mag range. Two of these detections were ~ 0.25 mag. brighter in the NUV.

In Figure 5 we show a concatenated series of 10 exposures (in the form of light-curves of NUV photon flux versus time) for this source. This plot represents the light-curves from all of the exposures strung together, and does not represent a contiguous time-series of observations. However, it is apparent that the overall flux level recorded over a total of $\sim 15,000$ s of observations (but in reality recorded over an actual period ~ 24 hours) is of a near-constant nature. We note that towards the end of the observational period there was a slow, but steady increase in activity (of $\sim 30\%$) for this source that was below the threshold of both of our variability detection techniques. The enhanced activity level is long-lived ($\gg 3000$ s) and thus when viewed over one exposure period the light-curve signature appears to be of a ‘quasi-constant’ nature. We believe that this type of light-curve is best explained as an extended period of repeated low-level flare activity following the short emission period of a large flare event (which unfortunately our *GALEX* observations missed). We shall return to the importance of this form of elevated activity in Section 4.4.

4.3.3. *Hyades-B source 04:26:04.4 +17:07:14.0*

This source was recognized as a flare star in the *ROSAT* X-ray survey of the Hyades (Stern et al. 1995). Its membership of the Hyades cluster has been confirmed by Leggett et al. (1994) who derive a distance of 46.8pc and they classify the star as a possible M-dwarf binary. Its associated NUV light curve is shown in Figure 4 for the flare event presently observed by *GALEX*. This event has a fast rise-time (~ 20 sec) followed by a ‘quasi-exponential’ decay, which also exhibits a secondary emission peak at time = 480 s. We note that the flare on this star was the largest of all 7 flare events observed with *GALEX* by an order of magnitude. This star was also observed in a second flare outburst, but with an intensity far smaller than the major event. This star has SDSS DR6.0 photometric colors indices of $(r - i) = 1.38$ and $(i - z) = 1.22$, which would suggest a spectral type of M3.5 to M6.5 (West et al. 2008).

In Figure 6 we show a more detailed plot of the NUV and associated FUV light-curves recorded by *GALEX* during the one exposure in which the large flare event occurred. It is clear that the FUV channel follows the same light-curve signature as the NUV channel. Within the measurement error of *GALEX* the start times of both the primary ($t \sim 180$ s) and secondary ($t \sim 490$ s) flare events are the same.

We have also plotted the ratio of FUV to NUV flux versus time for the same exposure period (i.e. a color ratio plot) in Figure 6. The photon count rates have been

converted to fluxes (in $\text{erg cm}^{-2} \text{s}^{-1} \text{\AA}^{-1}$) using the appropriate conversion factors for the *GALEX* instrument (Morrissey et al. 2005). This plot can be directly compared to the one shown in Figure 1 of Robinson et al. (2005) for the giant flare recorded by *GALEX* on the dM4e star GJ 3685A. In both cases the FUV/NUV ratio increases rapidly to values greater than unity, which is then followed by a period of exponential decay in which the NUV flux exceeds that of the FUV. Finally the flux ratio value rises above unity again as a second flare evolves (at $t \sim 490$ s). The classic explanation for such behavior is that FUV line emission (from CIV $\lambda 1550\text{\AA}$) dominates the early stages of flare evolution, which is subsequently followed by dominance by NUV line and/or continuum emission.

4.3.4. *Hyades-B source 04:27:33.6 +16:52:22.0*

This source is identified as the star Cl* Melotte 25 LH 110, with reported photometric magnitudes of $B=16.9$, $V=15.29$, $R=14.15$ and $J=10.9$ by Leggett & Hawkins (1988). These values are consistent with an M-type spectral classification for this star, as are its 2MASS colors listed in Table 1. The source also has SDSS DR6.0 photometry with color indices of $(r - i) = 1.15$ and $(i - z) = 1.12$, which would indicate a spectral type of M2.5 - M5.5 (West et al. 2008). The trigonometric distance for this M-type star is 26 pc, which would place it at the very periphery of the Hyades cluster whose stellar membership is thought to span the 25 - 65 pc distance range (Perryman et al. 1998). This star has not been listed as a possible Hyad member, since its proper motions of 2 mas yr^{-1} (RA) and -14 mas yr^{-1} (Dec) are inconsistent with Hyad cluster membership (Reid 1992).

In Figure 4 we show the photon flux as a function of time (recorded over one exposure period) for the observed flare on this source. To reveal the unusually active nature of this target, we also show the concatenated light-curves for all 10 exposures of this star in Figure 5. We see that in addition to the large flare at $t \sim 12000$ s there is also a far smaller flare event occurring at $t \sim 5500$ s. In addition, there is a period of enhanced UV activity starting at $t \sim 13700$ s. which is similar in nature to that discussed previously for the source Hyades-A 04:34:31.4 +17:22:20.1.

4.3.5. *Hyades-B source 04:28:42.7 +17:11:50.3*

The SDSS DR6.0 color indices for this star of $(r - i) = 1.71$ and $(i - z) = 1.01$ suggest a spectral type of M4 to M5 (West et al. 2008). There is no additional catalogue information for this star and thus we are unable to speculate whether it is a Hyad member and we therefore place a conservative distance estimate of 20 - 50 pc for this star.

The UV flare signature for this source shown in Figure 4 is very weak, and although of low S/N ratio, it appears to be quite a long-lived event with an extended period of activity lasting > 300 s.

4.3.6. *Pleiades-A source 03:42:35.6 +21:50:31.0*

This UV variable source is the star V614 Tau, which has a history of previous optical flare activity (Haro et al. 1982). Its NUV light-curve shown in Figure 4 is probably the most complex of all of the flares we have observed. Although of low S/N ratio, the data reveal two flare intensity peaks separated by ~ 40 s followed by a very extended period of diminishing activity that lasts at least 300 s. The rise time for the initial flare is > 50 s, which is unusually long compared with other

UV flare vents we have detected. We also note the statistically significant small ‘bump’ that occurs ~ 40 s prior to the onset of the first main flare event. Pre-cursor flares of this type have routinely been recorded on the Sun at both visible and X-ray wavelengths. A cluster membership probability has not been assigned to this star (Stauffer et al. 1991), and thus we place a conservative distance estimate for it of between 20 - 130 pc.

4.3.7. *Pleiades-B source 03:43:35.5 +26:21:31.1*

This variable source is the high proper motion star NLTT 11679 (173 mas yr^{-1}). Such a high value of proper motion value rules out its possible membership of the Pleiades cluster (Hambly et al. 1991). The NUV light curve (Flare 1) in Figure 4 is of a classic UV flare signature, with a fast rise time and ‘quasi-exponential’ decay that lasts ~ 150 s (Welsh et al. 2007). However, the second flare observed on this star (Flare 2, Figure 4) has a significantly different UV light-curve signature with a significantly extended period of activity following the main rise in flux. These two flare events occurred in consecutive orbits (~ 60 min apart), with the smaller flare event (Flare 2) being a pre-cursor to the larger flare. Immediately prior to the exposure that contained Flare 2, the star was in a quiescent state with $\text{NUV}_{mag} = 21.7$. We place a conservative distance estimate for this M-type star of between 20 - 50 pc.

4.3.8. *Pleiades-B source 03:44:26.4 +26:02:31.0*

This is the dMe flare star named MZ Tau which has been catalogued by Deacon & Hambly (2004) as a member of the Pleiades cluster based on proper motion studies. It has been observed to flare at visual wavelengths (Chavushian & Gharibjanian 1975), whereas our the ‘varpix’ plot of our UV data did not show any flaring signature. Instead, its UV variability was observed as a gradual increase in flux level during one exposure, with the majority of the remaining observations being at the lowest limit of our detectability. Immediately prior to the brightest exposure of $\text{NUV}_{mag} = 20.72$, the two preceding exposures were of $\text{NUV}_{mag} = 21.6$ and 21.9 . This flux variability behavior suggests that MZ Tau was in an increasing state of activity, presumably prior to a large flare event whose peak flux was missed by our observations.

4.3.9. *Pleiades-B source 03:45:03.8 +26:11:08.1*

This source was an outlier from the main group of probable M-stars shown in Figure 2, but had large errors on its 2MASS color indices. Also it was positioned to the right of the main M star grouping, as opposed to the other 3 outliers which were positioned to the left of the main group. We note that the USNO-B1.0 image of this source suggests that it may have a companion star, which may explain the anomalous 2MASS color indices. It remained beneath detection levels for all but 5 of the NUV exposures, and although no flare signature was observed in the ‘varpix’ light curve for this object, there was the sizable increase of $\Delta\text{NUV} = 2.17$ mag over its lowest observed magnitude (i.e. the largest magnitude variation in all of the Pleiades observations). There is no catalogued information for this star and thus we cannot assess whether it is a cluster member or not.

4.3.10. *Pleiades-B source 03:45:43.6 +26:05:05.0*

This star (CI* Melotte 22 SK 507) is listed as a non-member of the Pleiades cluster (Stauffer et al. 1991), based on its high

proper motion value. Its 2MASS colors are consistent with an M-type classification, and in Figure 4 its NUV light-curve shows a short ($t \sim 25$ s) rise-time flare event followed by an extended diminishing activity period lasting ~ 300 s. Although the data is of low S/N, this diminishing activity period seems to contain several small flare events occurring after the main flare event. No other data exists for this star, and we conservatively place a distance range of 20 - 80 pc for this dMe star.

4.4. Flare Energies

Estimates for the total NUV energy emitted from each of the 7 flare events listed previously are shown in columns 2 and 3 of Table 2. These estimates have been derived from subtracting the average of the integrated flux 200 s prior to the onset of the flare and then integrating the total emitted flux (shown in Figure 4) over the time period of the UV flare event. Unfortunately accurate distances are not available for all of the 6 stars that flared, and in Table 2 we place maximum and minimum estimates for these energies based on the distances given in the previous Section. For flare stars with known distances, the values in columns 2 and 3 are identical.

The flare energy values found for both clusters are all in the 2×10^{27} to 5×10^{29} erg range, which (on average) are \sim two orders of magnitude lower than that found in a *GALEX* survey of M star flares (Welsh et al. 2007). This level of flare energy is similar to that found in varying low-level emission activity in X-ray observations of the nearby dM5.5e flare star Proxima Cen (Gudel et al. 2004). Our detection of such low energy events can either be due to only small flares being produced on the dMe stars in both cluster fields, or that the Welsh et al. study was biased towards the detection of far more energetic events. We favor the latter interpretation, since in the Welsh et al. survey of UV flare events found in the (then) available *GALEX* data archive, they found an average change of $\Delta\text{NUV} = 2.7$ mag. for events on suspected dMe stars. If we presently restrict our selection of flare events to the 6 stars shown in Figure 4, then inspection of their NUV magnitudes listed in Table 1 reveals an average magnitude change of $\Delta\text{NUV} = 1.82$ mag. We note that the *GALEX* survey study of M-dwarf variability was performed using the ‘varpix’ software search set for a variability S/N ratio of $> 15:1$ (Welsh et al. 2007), thus biasing the detection of larger variable events than those of our present study. For the case of the 3 flare variable events found in the Hyades fields we derive an average magnitude change of $\Delta\text{FUV} > 1.39$ mag.

In Section 4.3.2 we noted that there was at least a > 3000 s period of enhanced UV activity on the Hyades-A source 04:34:31.3 +17:22:20.1. If we integrate the excess flux above that of the background level (shown as a dotted line in Figure 5) over one exposure period, we derive a total energy of 5.5×10^{27} to 3.4×10^{28} erg (assuming a minimum and maximum distance to the source of 20 - 50 pc). We note that this increase in energy is far greater than that attributed to the short period flare shown in the upper plot of Figure 5. This result is significant, since many of the M-type variables were observed in this ‘quasi-constant’ state of increased flux in addition to being observed in a classic flaring mode. Since these periods of increased activity last for significant time intervals, they would seem to be the major contributor of UV energy output for dMe stars. These observations thus raise the intriguing question as to which type of increasing flux versus time signature actually constitutes recognition as a flare event and which is the more important with regard to total energy output? Our present data would suggest that the periods of

increased NUV and FUV activity that have no accompanying classic flare signature may contribute a far larger energy output, and this discussed in more detail in Section 4.5.

4.5. Discussion

Unfortunately, our *GALEX* observations of both cluster fields have revealed only one dMe flare star (Hyades-B source 04:26:04.4 +17:07:14.0) as being a definite cluster member. Thus, we are presently unable to carry out a meaningful comparison of the UV activity of dMe star members in both clusters. Additionally, due to the uneven cadence observations made by the *GALEX* satellite, we believe that although the UV wavelength region is clearly ideally suited to the detection and observation of flares occurring on known dMe stars, the visible regime is currently better suited to assess chromospheric activity rates. Such optical observations should be carried out on large numbers of cluster members (whose proper motion, spectral type and distance have previously been determined) using sensitive H-alpha spectral measurements observed over more extended time periods (Reid et al. 1995; Stauffer et al. 1997). Furthermore, our UV observations have raised the question as to which type of increasing flux versus time signature actually constitutes recognition as a true flare event and which is the more important with regard to total UV energy output. For example, two sets of UV light-curves shown in Figure 5 may well be both associated with dMe stars but only one of the stars (Hyades-B 04:27:33.6 +16:52:22.2) can definitely be confirmed as being a flare star that exhibits a classic flare signature. The *GALEX* observations of the other star (Hyades-A 04:34:31.3 +17:22:20.1) revealed only periods of increased NUV and FUV activity with no actual (short-term) flare signature being recorded. However, the total energy output over one exposure period of increased UV activity was greater than that attributed to many classic short period flares. This latter observation concurs with X-ray data for other flare stars that suggest that there may not be a true quiescent state for dMe stars (Gudel et al. 2003). Instead, the observed low energy state may actually be a superposition of many small, but long lasting, flare events. Both X-ray and visible time-resolved spectra of flare events (Gudel et al. 2004; Fuhrmeister et al. 2008)) both show line and continuum emission variations that could generate the multiple peaks and substructure that we have observed in both our NUV and FUV light-curves. Clearly theorists need to fully explain which physical processes in the chromospheres and coronae on dMe stars that give rise to all of this substructure observed at different wavelengths. This may be relevant in explaining the difference in the shorter rise time of flares observed at visible wavelengths ($t \sim 10$ s) compared with those presently detected at UV wavelengths ($t \sim 50$ s).

5. CONCLUSION

We have presented a time-series of near and far ultraviolet imaging observations of four 1.2° diameter fields along sight-lines to the Hyades and Pleiades open clusters using the *GALEX* satellite to investigate possible UV variability of the stellar members. Stellar UV sources in each cluster field were extracted from each exposure image recorded over a total observing period of $\sim 15,000$ s, and their corresponding NUV and UV source magnitudes derived. These exposure-to-exposure source magnitudes were then queried to reveal

possible UV variability over the time-series of observations. In addition other time variability tests were carried out on the actual photon list data. These search methods revealed 16 UV variable sources, whose maximum and minimum variations in NUV and FUV source magnitudes are listed in Table 1.

The UV images of all 4 fields are dominated by the presence of bright (nearby) F and G field stars, with the Pleiades images showing UV emission in the form of filamentary structures due to the scattering and refraction of UV starlight by interstellar gas and dust grains.

We have used a 2MASS color-color indices plot to identify possible M-type stars from our list of 16 UV variables. This method revealed two G-type stars and one previously unknown RR Lyrae star (Hyades-B source 04:28:32.4 +16:58:21.6, with a derived period of 0.624 d and a distance of ~ 4.5 to 7 kpc), that were clearly separate from the remaining 13 variables whose spectral types were consistent with that of M stars. Of these 13 possible M-type stars we have detected 7 stellar flare events recorded towards 6 probable dMe stars. Light-curves (flux versus time) are presented for these 7 events. The majority of these M-type UV variable stars did not exhibit a 'classic' flare signature in plots of their UV flux versus time. Instead, these sources were observed during periods of near-constant but elevated levels of activity compared with exposure periods in which only lower flux levels were detected.

Energies for the 7 flare events have been derived from the photon flux versus time plots, using estimates of the distances to these sources. The maximum and minimum flare energies (based on the distance uncertainties) span the range 2×10^{27} to 5×10^{29} erg, which is about 2 orders of magnitude less than the average flare energy found in a survey of ~ 50 dMe stellar flares observed with *GALEX* (Welsh et al. 2007). This anomaly can be explained by the fact that in the latter study the software detection methods were biased towards the discovery of far larger flare events. In our present study of the two open clusters we find an average variability change of $\Delta\text{NUV} = 1.82$ mag for the six dMe flare stars over the 15,000 sec of observations. Rather surprisingly, only one of the flare events could be definitely associated with an outburst on a star that is a Hyades member (i.e. Hyades-B source 04:26:04.4 +17:07:14.0), with all the other flare events occurring on stars with indefinite cluster membership.

We gratefully acknowledge NASA's support for construction, operation and science analysis for the *GALEX* mission, developed in cooperation with the Centre National d'Etudes Spatiales of France and the Korean Ministry of Science and Technology. We acknowledge the dedicated team of engineers, technicians, and administrative staff from JPL/Caltech, Orbital Sciences Corporation, University of California, Berkeley, Laboratoire d'Astrophysique de Marseille, and the other institutions who made this mission possible. We also thank Suzanne Hawley and John Bochanski (University of Washington) and Andrew West (UC Berkeley) who gave excellent guidance and advice in writing this paper.

Financial support for this research was provided by the NASA *GALEX* Guest Investigator program, administered by the Goddard Spaceflight Center in Greenbelt, Maryland. This publication makes use of data products from the SIMBAD database, operated at CDS, Strasbourg, France.

REFERENCES

- Adams, J., Satuffer, J., Monet, D. et al., 2001, *AJ*, 121, 2053
 Ayres, T., Brown, A., Osten, R. et al., 2001, *ApJ*, 549, 554-
 Bertin, E. and Arnouts, S., 1996, *A & A*, 117, 393
 Chavushian, H. & Gharibjanian, A., 1975, *Astrophysics*, 11, 565
 Cutri, R.M. et al., 2003, 2MASS All Sky Catalog of Point Sources (The
 IRSA 2MASS All-Sky Point Source catalog, NASA/IPAC Infrared
 Science Archive. <http://irsa.ipac.caltech.edu/applications/Gator>)
 Deacon, N. & Hambly, N., 2004, *A&A*, 416, 125
 Dobbie, P., Kenyon, F., Jameson, R. et al., 2002, *MNRAS*, 329, 543
 Finlator, K., Ivezić, Z., Fan, X. et al., 2000, *AJ*, 120, 2615
 Fuhrmeister, B., Liefke, C., Schmitt, J. & Reiners, A., 2008, *A&A*, 487, 293
 Gibson, S. and Nordsieck, K., 2003, *ApJ*, 589, 347
 Gudel, M., Audard, M., Kashyap, V. et al., 2003, *ApJ*, 582, 423
 Gudel, M., Audard, M., Reale, F. et al., 2004, *A & A*, 416, 713
 Hambaryan, V., Mirzoyan, L., Wichmann, R. et al., 1997, *Astrophysics*, 40,
 354
 Hambly, N., Jameson, R. & Hawkins, M., 1991, *MNRAS*, 253, 1
 Haro, G., Chavira, E. & Gonzalez, G., 1982, *Bol. Inst. Tonantzintla*, 3, 3
 Hawley, S., Allred, M., Johns-Krull, C. et al., 2003, *ApJ*, 597, 535
 Leggett, S. and Hawkins, M., 1988, *MNRAS*, 234, 1065
 Leggett, S., Harris, H. and Dahn, C., 1994, *AJ*, 108, 944
 Martin, D.C., Fanson, J., Schiminovich, D., et al. 2005, *ApJ*, 619, L1
 Micela, G., Sciortino, S., Kashyap, V. et al., 1996, *ApJS*, 102, 75
 Mirzoyan, L., Ambaryan, V. and Garibdzhanyan, A., 1994, *Ap*, 37, 297
 Monet, D., Levine, S., Casian, B. et al., 2003, *AJ*, 125, 984
 Morrissey, P., Sciminovich, D., Barlow, T. et al., *ApJ*, 619, L7
 Morrissey, P., Conrow, T., Barlow, T. et al., 2007, *ApJS*, 173, 682
 Osten, R., Hawley, S., Allred, J. et al., 2005, *ApJ*, 621, 398
 Panagia, P. & Andrews, A., 1995, *MNRAS*, 277, 423
 Perryman, Brown, A., Lebreton, Y. et al., 1998, *A & A*, 331, 81
 Pillitteri, I., Micela, G., Reale, F. and Sciortino, S., 2005, *A & A*, 430, 155
 Reid, N., 1992, *MNRAS*, 257, 257
 Reid, N., Hawley, S. and Mateo, M., 1995, *MNRAS*, 272, 828
 Robinson, R., Wheatley, J., Welsh, B.Y. et al., 2005, *ApJ*, 633, 447
 Segura, A., Kasting, J., Meadows, V. et al., 2005, *AsBio*, 5, 706
 Soderblom, D., nelan, E., Benedict, G. et al., *AJ*, 129, 1616
 Sollima, A., Cacciari, C., Arkharov, A. et al., 2008, *MNRAS*, 384, 1583
 Stauffer, J., Klemola, A., Prosser, C. & Probst, R., 1991, *AJ*, 101, 980
 Stauffer, J., Balachandran, S., Krishnamurthi, A. et al., 1997, *ApJ*, 475, 604
 Stauffer, J., Hartmann, L., Fazio, G. et al., 2007, *ApJS*, 172, 663
 Stern, R., Schmitt, J. and Kahabka, P., 1995, *ApJ*, 448, 683
 Terndrup, D., Stauffer, J., Pinsonneault, M. et al., 2000, *AJ*, 119, 1303
 Welsh, B.Y., Wheatley, J., Heafield, K. et al., 2005, *AJ*, 130, 825
 Welsh, B.Y., Wheatley, J.M., Seibert, M. et al., 2007, *ApJS*, 173, 673
 West, A., Hawley, S., Walkowicz, L. et al., 2004, *AJ*, 128, 426
 West, A., Hawley, S., Bochanski, J. et al., 2008, *AJ*, 135, 785
 Wheatley, J.M., Welsh, B.Y., Siegmund, O. et al., 2005, *ApJ*, 619, L123
 Wheatley, J.M., Welsh, B.Y. and Browne, S.E., 2008, *AJ*, 136, 259
 York, D. G. et al., 2000, *AJ*, 120, 1579

TABLE 1
UV VARIABLE SOURCES

<i>GALEX</i> Field	R.A.(J2000)	Dec.(J2000)	FUV _{max}	FUV _{min}	NUV _{max}	NUV _{min}	Simbad Identification	(H - K)	(J - H)
Hyades-A	04:33:56.6	+16:52:09.6	22.71	>23.5	21.31	>22.5	Cl* Melotte 25 Reid 332	0.630	0.267
Hyades-A	04:34:31.3	+17:22:20.1	20.47	20.78	19.66	20.37	USNOB1.0 1073-0063497	0.265	0.706
Hyades-B	04:26:04.4	+17:07:14.0	18.14	20.47	17.56	21.67	Cl* Melotte 25 LH 129	0.289	0.611
Hyades-B	04:27:33.6	+16:52:22.2	21.38	22.17	20.18	20.91	Cl* Melotte 25 LH 110	0.225	0.639
Hyades-B	04:27:41.2	+16:33:09.4	21.61	>23.5	20.84	22.46	IRXS J042738.6+171837	0.573	0.268
Hyades-B	04:27:53.6	+16:51:36.0	22.98	23.36	20.49	21.17	USNOB1.0 1068-0045793	0.184	0.302
Hyades-B	04:28:32.4	+16:58:21.6	20.74	>23.5	19.30	20.94	USNOB1.0 1069-0046050	0.119	0.307
Hyades-B	04:28:42.7	+17:11:50.3	22.44	>23.5	21.39	22.50	SDSS J0422842.78+171149.6	0.323	0.666
Pleiades-A	03:42:35.6	+21:50:31.0	N/A	N/A	20.67	21.98	V614 Tau	0.188	0.672
Pleiades-A	03:42:36.9	+22:12:31.0	N/A	N/A	21.10	22.49	Cl* Melotte 22 LLP 137	0.337	0.570
Pleiades-B	03:42:59.0	+26:17:01.0	N/A	N/A	20.43	21.54	USNOB1.0 1162-0044156	0.341	0.113
Pleiades-B	03:43:35.5	+26:21:31.1	N/A	N/A	20.08	21.99	NLTT 11679	0.252	0.617
Pleiades-B	03:44:26.4	+26:02:31.0	N/A	N/A	20.72	21.99	MZ Tau	0.155	0.657
Pleiades-B	03:45:29.9	+26:26:12.0	N/A	N/A	20.76	21.75	USNOB1.0 1164-0045615	0.285	0.617
Pleiades-B	03:45:03.8	+26:11:08.1	N/A	N/A	20.24	22.41	2MASS 03450387+2611053	0.207	0.844
Pleiades-B	03:45:43.6	+26:05:05.0	N/A	N/A	20.61	22.37	Cl* Melotte 22 SK 507	0.277	0.555

TABLE 2
NUV FLARE ENERGIES

Flare Star	Flare Energy (max) (erg)	Flare Energy (min) (erg)
Hyades-B 04:26:04.4 +17:07:14.0	4.5E+29	4.5E+29
Hyades-B 04:27:33.6 +16:52:22.0	3.9E+27	3.9E+27
Hyades-B 04:28:42.7 +17:11:50.3	1.3E+28	2.3E+27
Pleiades-(A) 03:42:35.6 +21:50:31.0	1.1E+29	2.7E+27
Pleiades-(B) 03:43:35.5 +26:21:31.1	2.1E+28	3.4E+27
Pleiades-(B) 03:43:35.5 +26:21:31.1	1.8E+28	2.8E+27
Pleiades-(B) 03:45:43.6 +26:05:05.0	4.9E+28	3.1E+27

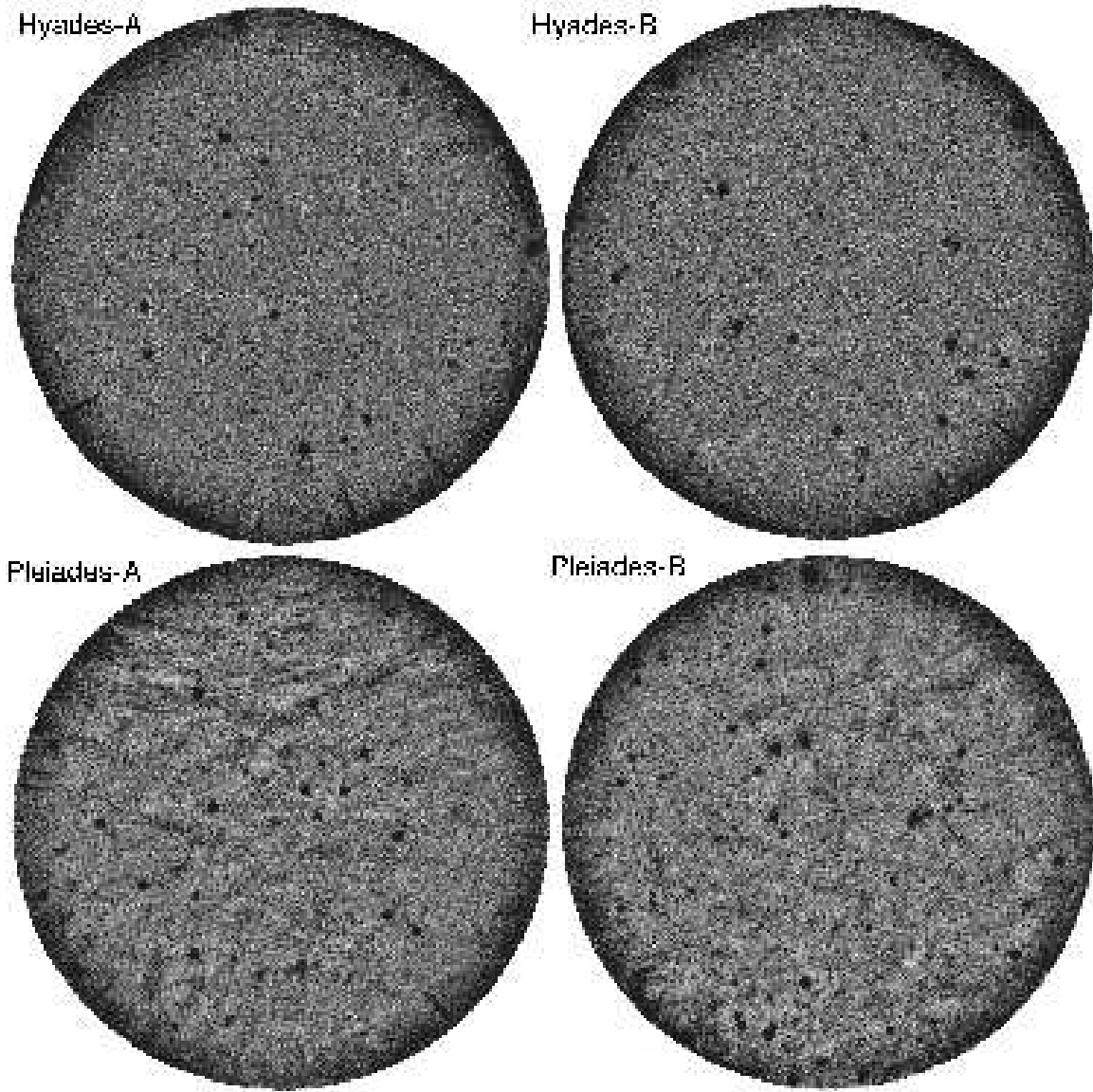


FIG. 1.— *GALEX* NUV images of the Hyades A & B and Pleiades A & B fields scaled to the same photon count rate. The streaks on the lower edge of the both Hyades images are due to scattered/reflected light from UV bright objects just beyond the nominal fields of view. Note the complexity of NUV emission from interstellar and nebular gas and dust in both Pleiades images.

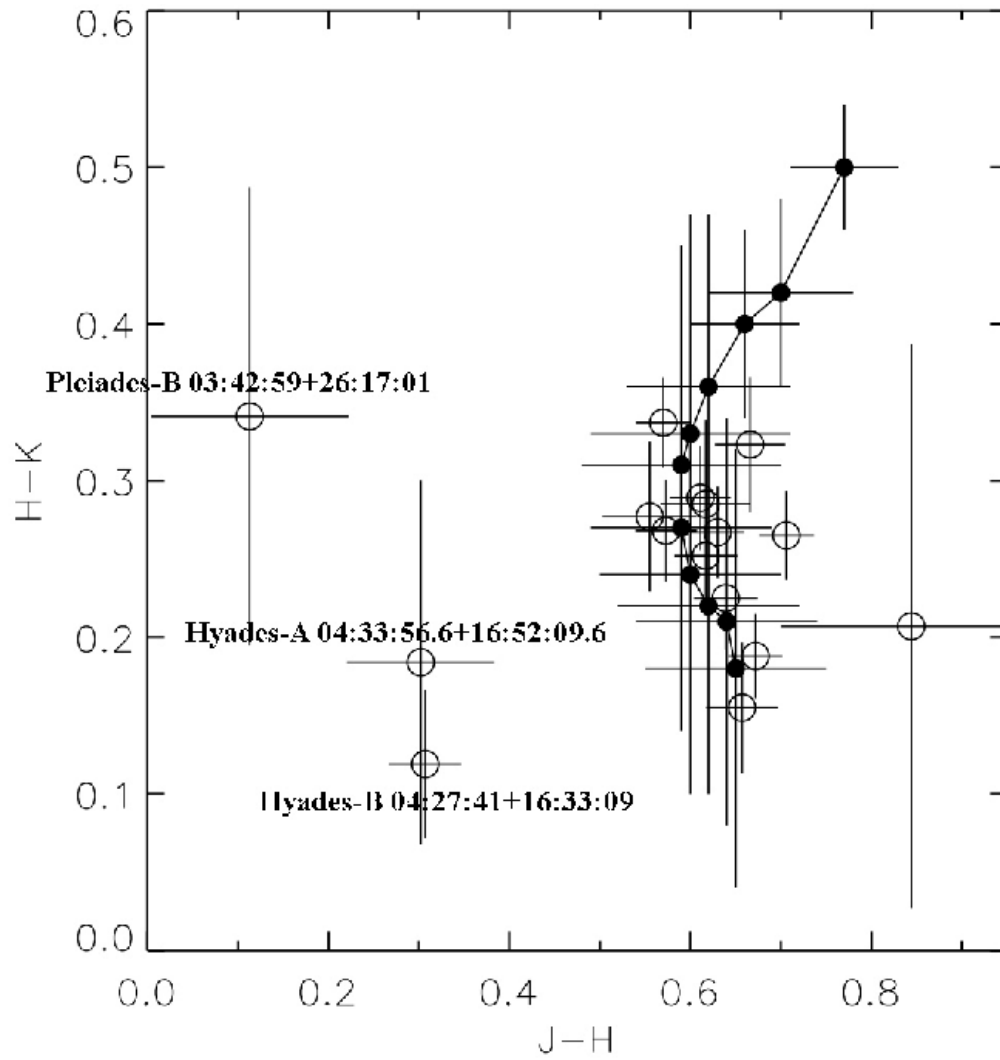


FIG. 2.— Plot of 2MASS $(H - K)$ versus $(J - H)$ color magnitudes for the 16 UV variable sources listed in Table 1 (open circles). Also shown is the locus of such color-color magnitudes for all 2MASS M0 to M9-type stars (filled circles) taken from West et al. (2008). Note that the majority of the UV variable sources lie within the color-color range for M-type stars.

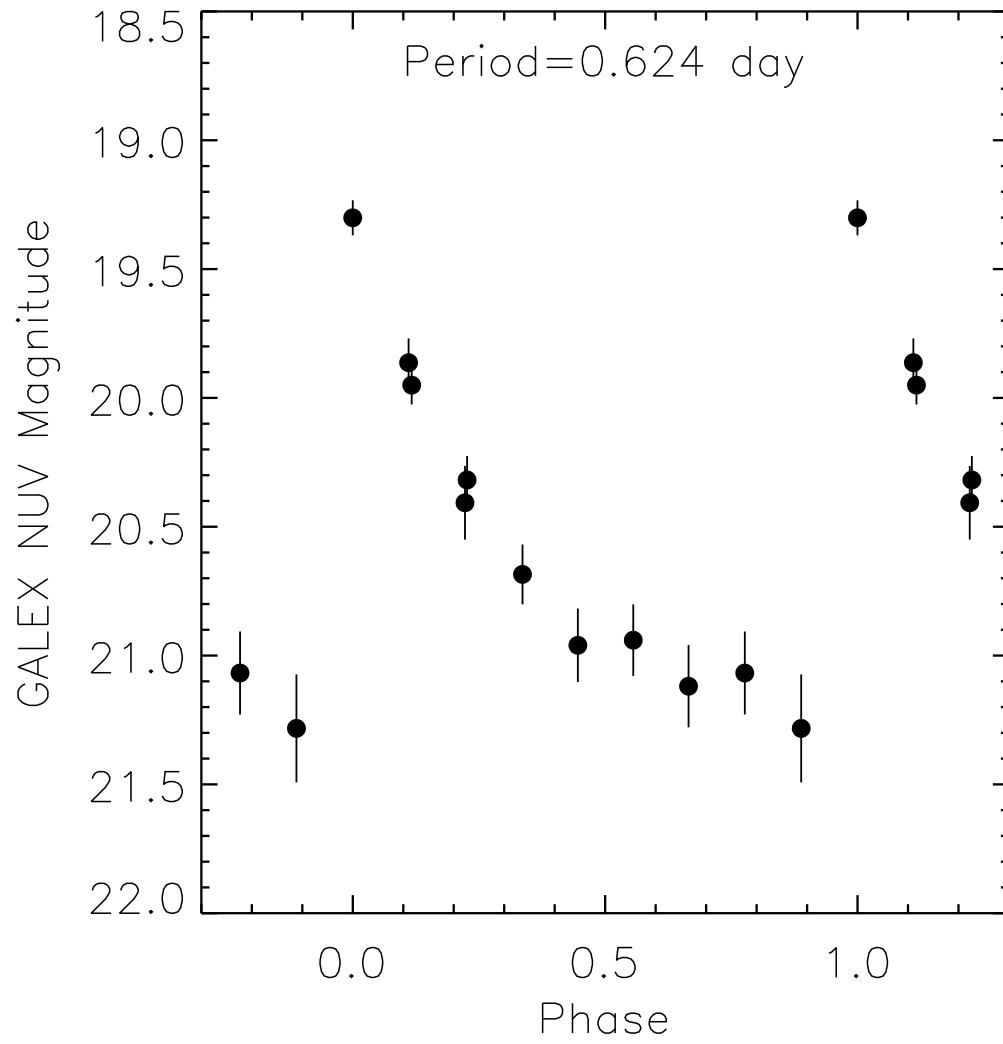


FIG. 3.— *GALEX* NUV light-curve for the Hyades-B source 04:28:32.4 +16:58:21.6. The best fit period for this RR Lyrae star is 0.624 d.

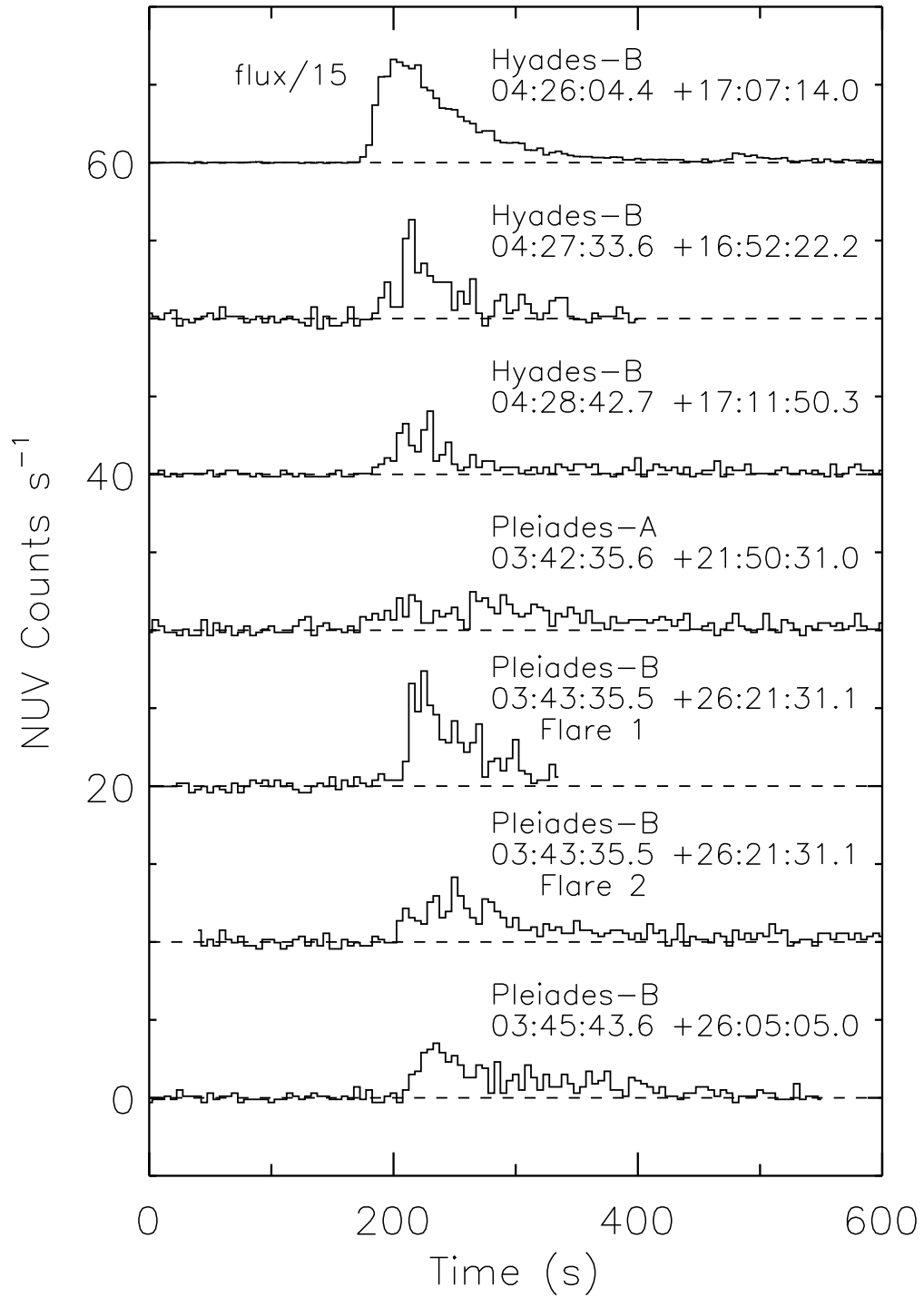


FIG. 4.— NUV light-curves (photon cts s^{-1} versus time) for the 6 objects that exhibited flaring signatures during the *GALEX* observations of the Hyades and Pleiades cluster fields.

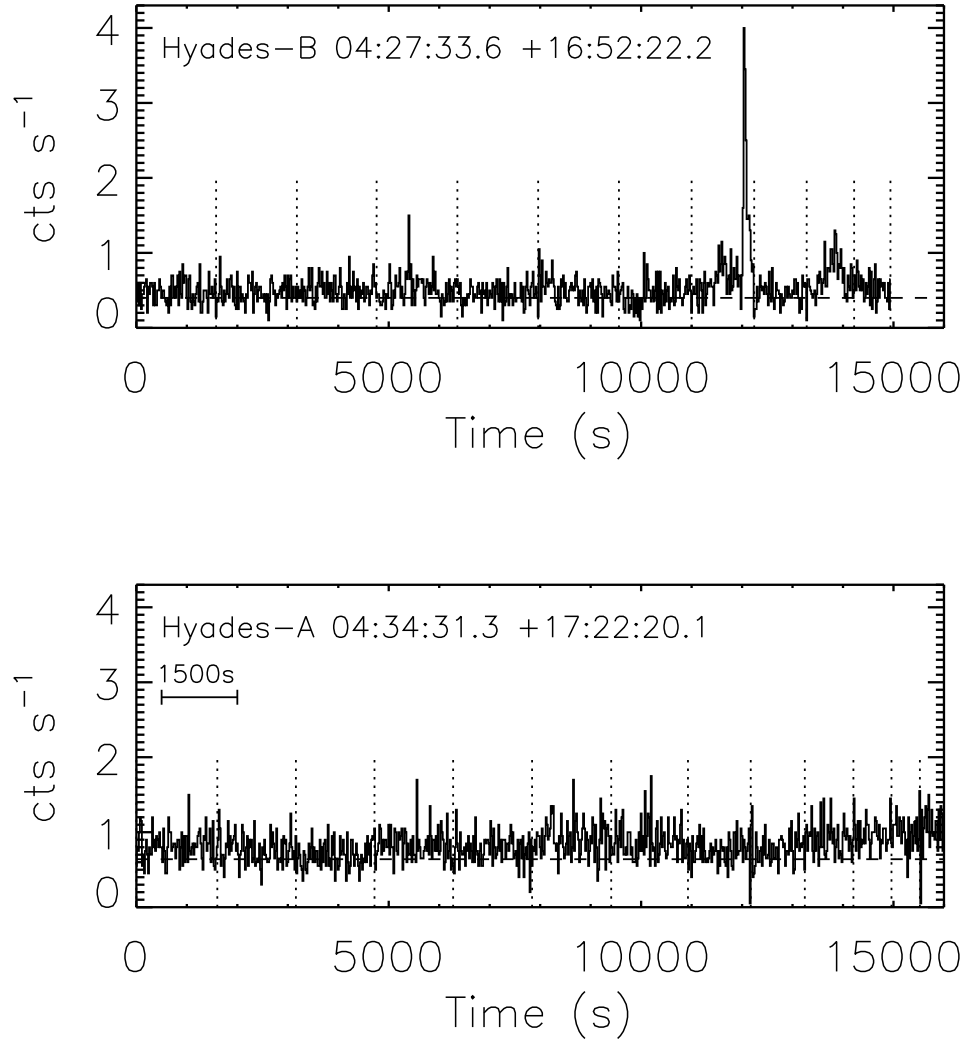


FIG. 5.— Concatenated series of 10 photon flux (cts s^{-1}) versus time light-curves (each of length ~ 1500 s) for two of the observed M-type sources. Significant gaps in time (due to satellite operational constraints) between each exposure are indicated by the dotted vertical lines. Note the large and far smaller short-term flare events on the upper plot. The source Hyades-A 04:34:31.3 +17:22:20.1 exhibits quasi-constant NUV emission for the majority of the exposure period, with a slowly increasing flux towards the last 3000 s of the exposures.

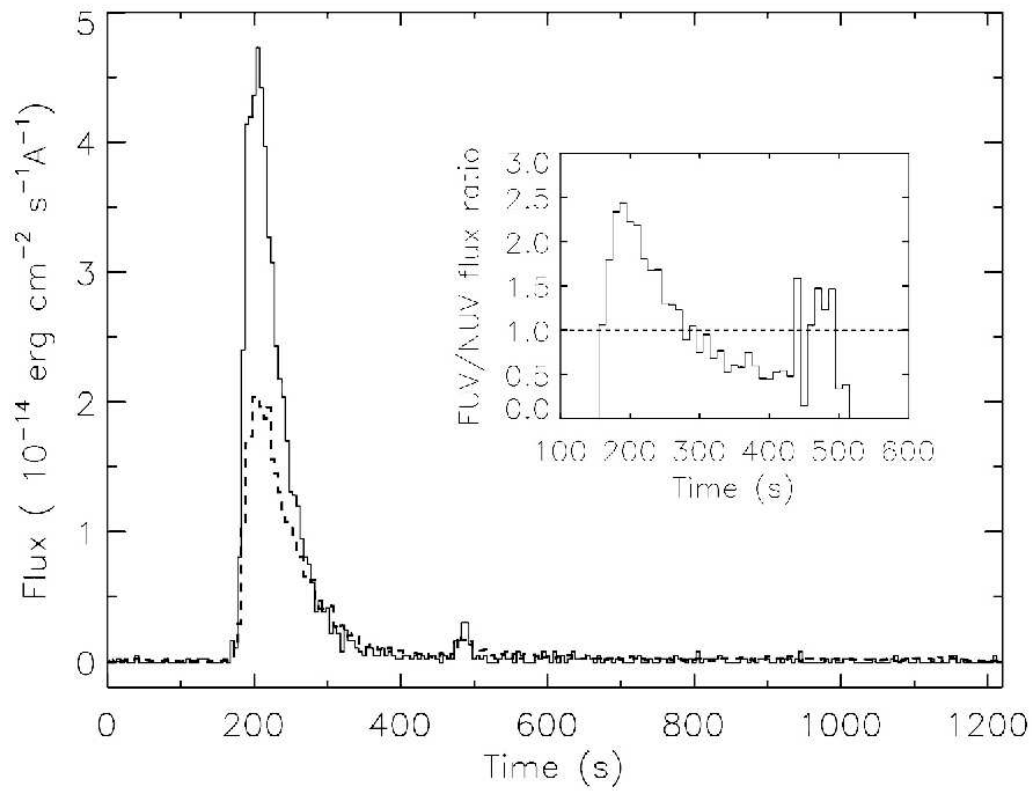


FIG. 6.— Comparison of the *GALEX* FUV (full line) and NUV (dashed line) light-curves for the flare event observed on Hyades-B source 04:26:04.4 +17:07:14.0. Inserted is a plot of the FUV/NUV flux ratio as a function of time over the same exposure period.